

## Dispersive Time-Delay Dynamical Systems

Alexander Pimenov,<sup>1,\*</sup> Svetlana Slepneva,<sup>2,3</sup> Guillaume Huyet,<sup>2,3,4,5</sup> and Andrei G. Vladimirov<sup>1,6</sup>

<sup>1</sup>Weierstrass Institute, Mohrenstraße 39, Berlin 10117, Germany

<sup>2</sup>Centre for Advanced Photonics and Process Analysis & Department of Physical Sciences,  
Cork Institute of Technology, Cork T12P928, Ireland

<sup>3</sup>Tyndall National Institute, University College Cork, Lee Maltings, Dyke Parade, Cork T12R5CP, Ireland

<sup>4</sup>National Research University of Information Technologies, Mechanics and Optics, 199034 Saint Petersburg, Russia

<sup>5</sup>Université Côte d'Azur, CNRS, Institut de Physique de Nice, Parc Valrose, 06108 Nice cedex 2, France

<sup>6</sup>Lobachevsky State University of Nizhny Novgorod, 23 Gagarina avenue, 603950 Russia

(Received 28 October 2016; revised manuscript received 28 March 2017; published 11 May 2017)

We present a theoretical approach to investigate the effect of dispersion in dynamical systems commonly described by time-delay models. The introduction of a polarization equation provides a means to introduce dispersion as a distributed delay term. The expansion of this term in power series, as usually performed to study the propagation of waves in spatially extended systems, can lead to the appearance of spurious instabilities. This approach is illustrated using a long cavity laser, where in the normal dispersion regime both the experiment and theory show a stable operation, while a modulation instability, commonly referred as the Benjamin-Feir instability, is observed in the anomalous dispersion regime.

DOI: 10.1103/PhysRevLett.118.193901

Time-delay dynamical systems (TDDS) have been successfully used to describe a variety of problems ranging from population and neural dynamics in biological sciences [1–3] to short pulse formation and the appearance of instabilities in laser physics [4–7]. They also appear in control [8], modeling of climate [9], modern computational methods [10,11], and the dynamics of coupled oscillators [12,13]. In each of these problems, delay is a direct consequence of wave propagation without dispersion. However, waves of different physical origin such as electromagnetic, acoustic, or water waves are subject to dispersion when propagating in a medium with the phase velocity depending on the frequency of the wave. In a nonlinear medium the interplay between dispersion and nonlinearity can give rise to a modulation instability [14] and soliton formation [15]. A commonly adopted approach to describe these phenomena is based on the application of nonlinear Schrödinger and complex Ginzburg-Landau (CGL)-type equations where the second and higher order chromatic dispersions are described by time derivatives of different orders. An important disadvantage of such models is that they assume the mean field approximation and are usually valid only in a small vicinity of the bifurcation point. Although TDDS are free from such limitations, an accurate mathematical description of the effect of dispersion of propagating waves in these models presents a big challenge. This Letter aims to close the gap and to provide a framework to study the effect of chromatic dispersion on the dynamics of TDDS. The dispersion is taken into account by introducing a distributed delay polarization term into the model equations. We show that unlike the Ginzburg-Landau type models where different-order dispersions are usually represented by the derivatives

of the corresponding orders, this term cannot be expressed as a power series of temporal derivatives, since any truncation of such an expansion leads to the appearance of a spurious instability. We apply the proposed framework to a ring laser incorporating a semiconductor amplifier as a gain medium and a long dispersive optical fiber delay line. Previously, we investigated experimentally the stability of this laser in the absence of dispersion and explained its behavior using a TDDS [16]. Here we observe a similar behavior both experimentally and numerically in the case of normal dispersion. On the contrary, in the case of anomalous dispersion we observe the appearance of a modulation instability similar to the Benjamin-Feir instability observed in the CGL equations.

Model equations of TDDS depend not only on the current state vector  $\mathbf{U}(t)$ , but also on the past states  $U_k(t - T_k)$ , where  $T_k$  are the delay times  $k = 1, \dots, n$ . Without the loss of generality we can assume that we have only a single delayed variable  $A(t - T) = U_1(t - T)$  and a single delay time  $T_1 = T$  in the model equations. The starting point of our analysis is based on the representation of TDDS as a one dimensional dynamical system where the variable  $a(t, z) = a(t - z/c, 0)$  is a solution of the unidirectional wave equation  $(1/c)a_t + a_z = 0$  on the interval  $0 \leq z \leq L$ , with  $A(t) \equiv a(t, 0)$  and  $A(t - T) \equiv a(t, L) = a(t - T, 0)$ . The dispersion is then introduced via a linear polarization term  $p(t, z)$  in the wave equation:

$$\frac{1}{c} \frac{\partial a}{\partial t} + \frac{\partial a}{\partial z} = p(t, z). \quad (1)$$

In the frequency domain  $\hat{p}$  is proportional to  $\hat{a}(\omega, z)$  via the susceptibility  $\chi(\omega, z)$  as

$$\hat{p}(\omega, z) = \chi(\omega, z)\hat{a}(\omega, z). \quad (2)$$

Equations (1) and (2) are integrated in the comoving reference frame ( $t' = t - z/c$  and  $z' = z$ ) to get  $\hat{a}(\omega, L)$

$$\hat{a}(\omega, L) = \hat{a}(\omega, 0)e^{\int_0^L \chi(\omega, z) dz}, \quad (3)$$

and  $a(t, L)$  is obtained by performing the inverse-Fourier transform of (3).

In this Letter, we assume that  $\chi(\omega, z) = \chi(\omega)$  is homogeneous in  $z$ ; hence, without loss of generality  $\chi(\omega)$  can be decomposed in a sum of Lorentzians

$$\chi(\omega) = - \int \frac{n(\omega_0)}{\Gamma(\omega_0) + i(\omega + \omega_0)} d\omega_0, \quad (4)$$

where  $n(\omega_0)$  is the density of states.

For a single Lorentzian,

$$\chi(\omega) = \frac{-\sigma}{\Gamma + i(\omega + \Omega)}, \quad (5)$$

with central frequency  $\Omega$  and full-width at half-maximum  $\Gamma$ , corresponding to  $n(\omega_0) = \sigma\delta(\omega_0 - \Omega)$ , one can write

$$a(t, L) = a(t - T, 0) + P(t - T) = A(t - T) + P(t - T), \quad (6)$$

where

$$P(t) = -\sigma L \int_{-\infty}^t e^{-(\Gamma+i\Omega)(t-s)} \frac{J_1[\sqrt{4\sigma L(t-s)}]}{\sqrt{\sigma L(t-s)}} A(s) ds. \quad (7)$$

The relation (6) gives an expression for the output field from the dispersive delay line. Therefore, in order to account for the effect of dispersion in the model equations we need to replace in these equations the output field  $A(t - T)$  from a dispersionless delay line with that calculated in the presence of chromatic dispersion:  $A(t - T) + P(t - T)$ . The resulting set of equations with distributed delay describes the behavior of the TDDS in the presence of dispersion and the usual tools of nonlinear dynamics theory can be applied to study the stability and bifurcations of various solutions.

We note that if we decompose the exponent in (3) in a power series at the point  $\omega = 0$  near the central frequency of our TDDS, then the truncation of this series at some  $N \geq 0$  leads to dispersion in the form  $P(t) = \sum_0^N \beta_n A^{(n)}(t)$ . Here  $\beta_n$  describes the effect of the  $n$ th order dispersion near the central frequency. Since polarization  $P(t)$  appears as a delay term in Eq. (6), the highest order delayed derivative arises from the  $N$ th order dispersion term of the expansion. This results in equations with delayed highest derivative formally equivalent to equations with negative delay (time advance), which break the causality principle and are known to exhibit spurious instabilities.

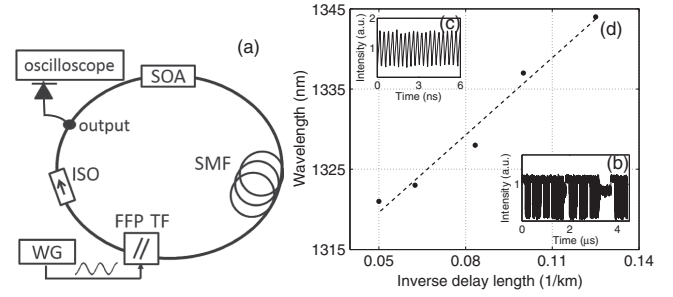


FIG. 1. (a) Experimental setup of the ring laser. SOA, semiconductor optical amplifier; ISO, isolator; SMF, single mode fiber; FFPTF, fiber Fabry-Pérot tunable filter; WG, waveform generator. (b) Bistability between the chaos and cw observed in the case of the normal dispersion. (c) Chaotic dynamics observed in the case of the anomalous dispersion. (d) Threshold division for the modulational instability for various fiber lengths: the bistability regime is observed to the right of the threshold line and chaos to its left.

To illustrate the application of our method to a specific physical problem, we shall now consider the example of a fiber ring laser incorporating a semiconductor optical amplifier and a tunable filter, as shown in Fig. 1(a). The influence of the dispersion was investigated by varying the filter transmission wavelength from 1280 to 1360 nm and the fiber length from 17 m to 20 km. The laser dynamics was analysed by a dc-coupled broadband 12 GHz photo-receiver and a real time oscilloscope of 12 GHz bandwidth.

When the laser operated in the normal dispersion regime (i.e., wavelengths below 1317 nm), the laser exhibited a behavior similar to that experimentally observed and theoretically explained in the dispersion free regime [16]. In short, we could observe continuous wave (cw), chaotic outputs, and random switching between these solutions for the same set of parameters as shown in Fig. 1 inset (b). A minor redshift of the filter transmission stabilized the cw solution while a blueshift destabilized the cw solution and generated a chaotic output. This asymmetry is apparent in Fig. 2(a) where the filter transmission wavelength is periodically modulated at a slow frequency (100 mHz). The laser displayed chaotic oscillations when the filter is blueshifted and a series of jumps between cw solutions when the filter is redshifted.

When the laser was set to operate in the anomalous dispersion regime, only chaotic oscillations occurred as shown in Fig. 1 inset (c), which were not influenced by any slight variations of the filter transmission wavelength. When the filter was quasistatically tuned, the laser output showed a strong dependence on the filter speed: at a slow modulation frequency the laser exhibited chaotic output regardless of the sweep direction [Fig. 2(b)] while as the filter modulation frequency increased, an asymmetry appeared [Fig. 2(c)]; however, the cw output had never been observed.

To further investigate the influence of the dispersion on the laser stability, we measured the wavelength at which the

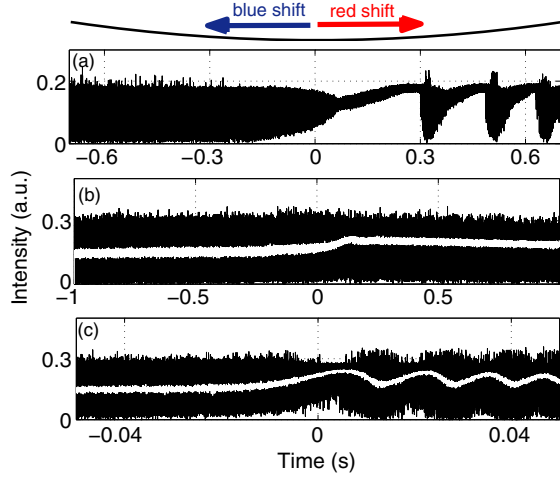


FIG. 2. Experimentally measured dynamics of the laser operating in a quasistatic regime at the turning point of the filter transmission wavelength (top curve) for the case of (a) the normal dispersion region (tuning around 1303 nm, 100 MHz modulation frequency); (b) the anomalous dispersion region (tuning around 1328 nm, 200 MHz modulation frequency); (c) the anomalous dispersion region (1600 MHz modulation frequency). Black: the intensity measured with 12 GHz bandwidth, white: the numerically filtered intensity.

transition from the bistable to chaotic dynamics occurred as a function of the cavity length and observed that the instability threshold is inversely proportional to the fiber length as shown on Fig. 1(d).

To theoretically describe this experiment, we added chromatic dispersion as a detuned Lorentzian absorption line to the time-delayed equations described in [16]. By following the formalism described above, we obtain the following equations:

$$\frac{dA}{dt} + (\gamma - iw)A = \gamma\sqrt{\kappa}e^{(1-i\alpha)G/2}[A_T + P_T], \quad (8)$$

$$\frac{dG}{dt} = \gamma_g[g_0 - G - (e^G - 1)|A_T + P_T|^2], \quad (9)$$

where  $A_T = A(t - T)$ ,  $P_T = P(t - T)$  is defined by (7),  $T$  is the cold cavity round trip time,  $\gamma$  is the tunable filter width,  $w$  is the relative position of the central frequency of this filter. The parameters  $\kappa$ ,  $\alpha$ , and  $g_0$  describe, respectively, the attenuation factor related to nonresonant loss per cavity round trip, linewidth enhancement factor, and the pump parameter. In the case of zero dispersion  $P = 0$  the DDE system (8) and (9) contains a single discrete delay and coincides with model equations studied in [16,17]. The normal dispersion regime corresponds to  $\Omega > 0$  in (5) and the anomalous dispersion to  $\Omega < 0$ .

To investigate theoretically the appearance of modulational instability in the system (8), (9), and (7) let us consider a cw solution in the form  $A(t) = A_0 e^{i\nu t}$  and  $G(t) = G_0$ , which together with (7) imply  $P(t) = (e^{-\sigma L/[\Gamma+i(\Omega+\nu)]} - 1)A_0 e^{i\nu t}$ . Following the approach

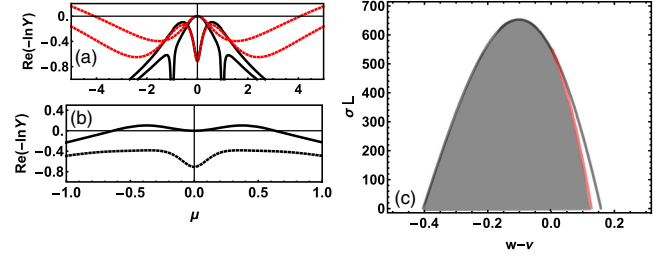


FIG. 3. (a) Real parts of two branches of the pseudocontinuous spectrum  $\text{Re}\Lambda_{\pm}(\mu)$  in the case of weak normal dispersion (7) (black line) and for dispersion decomposed up to second order  $P(t) = \beta_0 A(t) + \beta_1 A'(t) + \beta_2 A''(t)$  (light-colored line). Here,  $\beta_n \approx [-\sigma/(\Gamma + i\Omega)]^n$ , and  $\Omega = -1$ ,  $\sigma L = 0.2$ ,  $\Gamma = 0.01$ . (b)  $\text{Re}\Lambda_{\pm}(\mu)$  in the case of strong anomalous dispersion,  $\Omega = -13$ ,  $\sigma L = 1000.0$ ,  $\nu = 0$ . (c) Modulational instability boundary (black) and Turing-like instability [16] boundary (light or red color) in the anomalous dispersion regime on the plane of two parameters, dispersion strength  $\sigma L$  and the relative frequency of the cw regime  $w - \nu$ . The gray region denotes stable cw solutions. Other parameter values:  $\gamma = 1$ ,  $g_0 = 3.0$ ,  $\alpha = 2$ ,  $\kappa = 0.2$ ,  $\gamma_g = 0.1$ ,  $w = 0$ , and  $\Gamma = 0.001$ .

described in [18] we perform linear stability analysis of cw solutions  $A_0$ ,  $G_0$  in the limit  $T \rightarrow \infty$ . We linearize the system near the steady state  $A = (A_0 + \delta A e^{\lambda t})e^{i\nu t}$ ,  $G = G_0 + \delta G e^{\lambda t}$ , and  $P_1 = (P_0 + \delta P e^{\lambda t})e^{i\nu t}$ , with the relation  $\delta P = \delta A(e^{-\sigma L/[\Gamma+\lambda+i(\Omega+\nu)]} - 1)$  following from (7). Then we get a quadratic characteristic equation for the quantity  $Y = e^{-\lambda T}$  with the coefficients depending on  $\mu = \text{Im}\lambda$  in the limit  $T \rightarrow \infty$  [18,19]. Two branches of pseudocontinuous spectrum are obtained from the two solutions  $Y = Y_{\pm}$  of the characteristic equation  $\Lambda_{\pm}(\mu) = \text{Re}(-\ln Y_{\pm})$ . These branches are shown in Figs. 3(a) and 3(b) (black curves) indicating the presence of modulational instability in the anomalous dispersion regime in Fig. 3(b). Note that if we expand polarization (7) in the series of time derivatives and truncate this expansion at any  $N > 1$ , we observe the appearance of spurious instability [see Fig. 3(a), light-colored curves].

In the absence of dispersion ( $\sigma L = D_2 = 0$ ) a cw solution is always stable with respect to modulational instability when the central frequency of the spectral filter is tuned exactly to the frequency of this solution,  $w = \nu$  [ $(-1/\gamma^2) < 0$ ] [16]. In the case of dispersive delay line  $\sigma > 0$ , the necessary condition for the modulational instability at  $w = \nu$  is obtained from the relation  $(d^2 \text{Re}\Lambda_{+}/d\mu^2)(0) = 0$  as [19]

$$\alpha L D_2 < -\frac{1}{\gamma^2}, \quad (10)$$

where the second-order dispersion coefficient per unit length is given by

$$D_2 = \text{Im} \frac{d^2}{d\nu^2} \left( \frac{-\sigma}{\Gamma + i(\Omega + \nu)} \right).$$

This condition resembles the modulational instability criterion for the complex Ginzburg-Landau equation [20]. The sign of the second-order dispersion coefficient  $D_2$  is determined by the sign of  $\Omega$  for large enough  $|\Omega| > \Gamma\sqrt{3}$ . In particular, modulational instability (10) at  $w = \nu$  occurs only for the case of anomalous dispersion  $\Omega < 0$ . Moreover, condition (10) predicts the instability threshold for any second-order dispersion  $D_2$  to be inversely proportional to the fiber length  $L$ , which corresponds to the experimentally observed relation [see Fig. 1(d)].

We note that one can adiabatically eliminate carrier density and obtain in the limit of small field intensity a field equation with delayed cubic nonlinearity, where the modulational instability condition also takes the form (10) for  $w = \nu$ . Moreover, this condition holds for the Stuart-Landau equation under delayed dispersive feedback, which can be considered as a generic model describing the interplay of the nonlinearity and the feedback

$$\frac{dA}{dt} = (c + iw)A - (1 + i\alpha)A|A|^2 + \gamma e^{i\phi}[A_T + P_T], \quad (11)$$

where  $c > 0$ .

Stability analysis of the cw solution for various values of  $w - \nu$  in the static regime  $w = \text{const}$  allows us to understand the asymmetry of the dynamical output of the laser with respect to the sweeping direction in the quasistatic and Fourier domain mode-locking regimes [16]. Indeed, in the case of moderate normal or weak anomalous dispersion [see Fig. 3(c)], similarly to the case without dispersion, for  $w > \nu$  we observe a Turing-type instability of the cw solution, which leads to a jump from one longitudinal mode to another for positive sweep direction, whereas for  $w < \nu$  and a sufficiently high  $\alpha$  factor, the cw regime loses stability via a weak modulational instability, which results in the chaotic output of the laser for the negative sweep direction [16]. One can see from Fig. 3(c) that, when the strength of the anomalous dispersion  $d$  is increased above a certain threshold, the Turing-type instability at  $w > \nu$  is replaced by modulational instability, so that for both signs of the detuning  $w - \nu$  the cw solution is destabilized via a modulational instability. With a further increase of the dispersion strength, two modulational instability boundaries in Fig. 3(c) merge with one another and the cw regime becomes always unstable for any values of  $w - \nu$ .

To investigate the effect of anomalous dispersion on the dynamics of the ring laser in the quasistatic regime numerically, we assumed that the central frequency of the filter is swept periodically in time,  $w = w(t) = \Delta \sin \rho t$  [16], where  $\rho \ll 1$ . The effect of dispersion on symmetry properties of the ring laser output with respect to the sweep direction is illustrated by Fig. 4. In particular, it can be seen from Fig. 4(c) that for  $\sigma L = 600\gamma$ , when the small interval of detunings  $w - \nu$ , where the cw regime is stable, is limited by two modulational instability points [see Fig. 3(b)], a

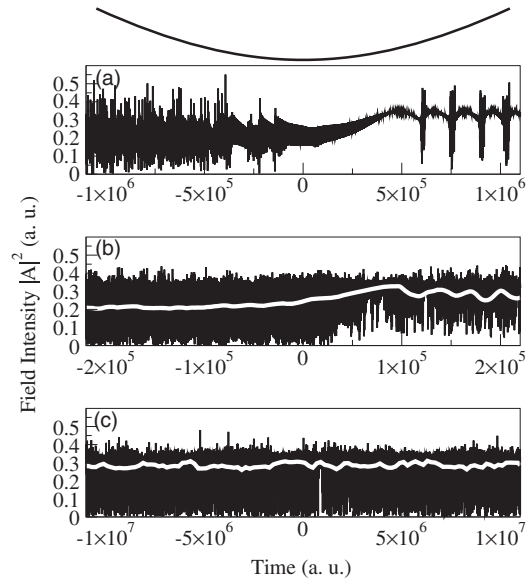


FIG. 4. Numerical solution of the system (8)–(9), (7) for  $\Delta(t) = \Delta_0 \sin \rho t$  at the turning point of the filter transmission  $\sin \rho t = -1$  (top) in case of (a) normal dispersion  $\Omega = 13$  (modulation frequency  $\rho = 10^{-6}$ ); (b) anomalous dispersion  $\Omega = -13$  (modulation frequency  $\rho = 5 \times 10^{-6}$ ); (c) anomalous dispersion  $\Omega = -13$  and modulation frequency  $\rho = 10^{-7}$ . The black traces are the recorded time traces and the white traces are numerically filtered signals. Here,  $\sigma L = 600$ ,  $\Delta = 5$ , and other parameters are as in Fig. 3.

chaotic output is observed for both sweep directions at low sweep speed  $\rho = 10^{-7}$ . On the contrary, for higher sweep speed  $\rho = 5 \times 10^{-6}$  one can see a weak attraction towards a cw regime and corresponding jumps in the numerically filtered field intensity  $|A|^2(t)$ , see Fig. 4(b). Thus, our numerical results are in good qualitative agreement with the experimental results presented in Fig. 2. Moreover, we could observe chaotic output in the anomalous dispersion regime with clear jumps in the numerical signal [see Fig. 4(b)] only for the dispersion strength such that the cw regime is weakly stable [see Fig. 3(c)]. For weaker dispersion we observe numerical time traces similar to Fig. 4(a), whereas for stronger dispersion the jumps become irregular. Therefore, we conclude that the corresponding experimental behavior [see Fig. 2(c)] could also be related to the existence of weakly stable cw states that are not observed in the static regime.

To conclude, we have provided a theoretical framework to describe the effect of dispersion in a nonlinear system modeled by a set of DDEs. This approach was successfully applied to describe the emergence of modulation instability observed experimentally in a ring cavity laser containing a long fiber delay line. In particular, we have shown that in the anomalous dispersion regime the dispersion of the fiber delay line can destabilize the cw laser operation leading to a turbulent behavior. This framework could be used to investigate the impact of dispersion on the dynamics of a broad

class of systems commonly described by DDEs. For example, this approach could be used to understand the effect of linear chromatic dispersion on the characteristics of the mode-locked regime in monolithic multisection lasers and other nonlinear photonic devices [6,7,10,21–26]. In particular, taking chromatic dispersion into consideration is unavoidable when modeling soliton mode-locked lasers frequently used for generation of femtosecond pulses [27], photonic crystal mode-locked lasers [25], as well as many other fiber, solid state, and semiconductor [28] optical systems. Using the asymptotic techniques described in [29] and integrating, by parts, Eq. (7) in the weak dispersion regime the laser DDE model and the Stuart-Landau equation can be reduced near the instability point of trivial zero intensity solution to the paradigmatic Ginzburg-Landau equation, which (unlike the equation derived in [29]) can demonstrate a dispersion induced modulational instability. This means that the turbulent behavior discussed above is a general phenomenon in many dispersive nonlinear systems exhibiting an Andronov-Hopf bifurcation and does not depend on the properties of a particular system under consideration.

The authors thank Sergio Rica, Stephen P. Hegarty, Julien Javaloyes, Svetlana Gurevich, Shalva Amiranashvili, and Dmitry Turaev for fruitful discussions and useful advice. A. P. and A. G. V. acknowledge the support of SFB 787 of the DFG. A. G. V. acknowledges the support of Grant No. 14-41-00044 of the Russian Science Foundation. G. H. acknowledges the Science Foundation Ireland under Contract No. 11/PI/1152. S. S. gratefully acknowledges the support of the EU FP7 Marie Curie Action FP7-PEOPLE-2010-ITN through the PROPHET project, Grant No. 264687.

\*Corresponding author.

alexander.pimenov@wias-berlin.de

- [1] T. Erneux, *Applied Delay Differential Equations* (Springer Science & Business Media, New York, 2009), Vol. 3.
- [2] S. A. Campbell, in *Handbook of Brain Connectivity* (Springer, Berlin, Heidelberg, 2007), pp. 65–90.
- [3] H. Smith, *An Introduction to Delay Differential Equations with Applications to the Life Sciences* (Springer Science & Business Media, New York 2010), Vol. 57.
- [4] A. G. Vladimirov and D. Turaev, Model for passive mode locking in semiconductor lasers, *Phys. Rev. A* **72**, 033808 (2005).
- [5] R. Lang and K. Kobayashi, External optical feedback effects on semiconductor injection laser properties, *IEEE J. Quantum Electron.* **16**, 347 (1980).
- [6] M. Marconi, J. Javaloyes, S. Barland, S. Balle, and M. Giudici, Vectorial dissipative solitons in vertical-cavity surface-emitting lasers with delays, *Nat. Photonics* **9**, 450 (2015).
- [7] A. Pimenov, V. Z. Tronciu, U. Bandelow, and A. G. Vladimirov, Dynamical regimes of a multistripe laser array with external off-axis feedback, *J. Opt. Soc. Am. B* **30**, 1606 (2013).
- [8] K. Pyragas, Continuous control of chaos by self-controlling feedback, *Phys. Lett. A* **170**, 421 (1992).
- [9] H. Kaper and H. Engler, *Mathematics and Climate* (SIAM, Philadelphia, 2013), Vol. 131.
- [10] D. Brunner, M. C. Soriano, C. R. Mirasso, and I. Fischer, Parallel photonic information processing at gigabyte per second data rates using transient states, *Nat. Commun.* **4**, 1364 (2013).
- [11] T. Nitta, *Complex-Valued Neural Networks: Utilizing High-Dimensional Parameters: Utilizing High-Dimensional Parameters* (IGI Global, Hershey, PA, 2009).
- [12] G. Kozyreff, A. G. Vladimirov, and P. Mandel, Global Coupling with Time Delay in an Array of Semiconductor Lasers, *Phys. Rev. Lett.* **85**, 3809 (2000).
- [13] B. Kelleher, C. Bonatto, P. Skoda, S. P. Hegarty, and G. Huyet, Excitation regeneration in delay-coupled oscillators, *Phys. Rev. E* **81**, 036204 (2010).
- [14] H. C. Yuen and B. M. Lake, Instabilities of waves on deep water, *Annu. Rev. Fluid Mech.* **12**, 303 (1980).
- [15] V. E. Zakharov and A. B. Shabat, Exact theory of two-dimensional self-focusing and one-dimensional self-modulation of waves in nonlinear media, *Sov. Phys. JETP* **34**, 62 (1972).
- [16] S. Slepneva, B. Kelleher, B. O’Shaughnessy, S. Hegarty, A. G. Vladimirov, and G. Huyet, Dynamics of Fourier domain mode-locked lasers, *Opt. Express* **21**, 19240 (2013).
- [17] S. Slepneva, B. O’Shaughnessy, B. Kelleher, S. Hegarty, A. G. Vladimirov, H. Lyu, K. Karnowski, M. Wojtkowski, and G. Huyet, Dynamics of a short cavity swept source OCT laser, *Opt. Express* **22**, 18177 (2014).
- [18] S. Yanchuk and M. Wolfrum, A multiple time scale approach to the stability of external cavity modes in the Lang-Kobayashi system using the limit of large delay, *SIAM J. Appl. Dyn. Syst.* **9**, 519 (2010).
- [19] See Supplemental Material at <http://link.aps.org/supplemental/10.1103/PhysRevLett.118.193901> for the technical details on the stability analysis of the delayed model for a ring laser.
- [20] W. van Saarloos and P. Hohenberg, Fronts, pulses, sources and sinks in generalized complex Ginzburg-Landau equations, *Phys. D* **56**, 303 (1992).
- [21] E. Turitsyna, S. Smirnov, S. Sugavanam, N. Tarasov, X. Shu, S. Babin, E. Podivilov, D. Churkin, G. Falkovich, and S. Turitsyn, The laminar-turbulent transition in a fibre laser, *Nat. Photonics* **7**, 783 (2013).
- [22] S. Boscolo, S. V. Sergeyev, C. Mou, V. Tsaturian, S. Turitsyn, C. Finot, V. Mikhailov, B. Rabin, and P. S. Westbrook, Nonlinear pulse shaping and polarization dynamics in mode-locked fiber lasers, *Int. J. Mod. Phys. B* **28**, 1442011 (2014).
- [23] M. Marconi, J. Javaloyes, S. Balle, and M. Giudici, How Lasing Localized Structures Evolve out of Passive Mode Locking, *Phys. Rev. Lett.* **112**, 223901 (2014).
- [24] B. Garbin, J. Javaloyes, G. Tissoni, and S. Barland, Topological solitons as addressable phase bits in a driven laser, *Nat. Commun.* **6**, 5915 (2015).

- [25] M. Heuck, S. Blaaberg, and J. Mørk, Theory of passively mode-locked photonic crystal semiconductor lasers, *Opt. Express* **18**, 18003 (2010).
- [26] L. Jaurigue, E. Schöll, and K. Lüdge, Suppression of Noise-Induced Modulations in Multidelay Systems, *Phys. Rev. Lett.* **117**, 154101 (2016).
- [27] J. N. Kutz, Mode-locked soliton lasers, *SIAM Rev.* **48**, 629 (2006).
- [28] R. Paschotta, Soliton-like pulse-shaping mechanism in passively mode-locked surface-emitting semiconductor lasers, *Appl. Phys. B* **75**, 445 (2002).
- [29] T. Kolokolnikov, M. Nizette, T. Erneux, N. Joly, and S. Bielawski, The  $Q$ -switching instability in passively mode-locked lasers, *Physica (Amsterdam)* **219D**, 13 (2006).